

Terpolymerization of Acrylamide, Acrylic Acid, and Acrylonitrile: Synthesis and Properties

ISMAIL MATHAKIYA, VEENA VANGANI, ANIMESH KUMAR RAKSHIT

Chemistry Department, Faculty of Science, M.S. University, Baroda 390002, India

Received 27 May 1997; accepted 3 September 1997

ABSTRACT: Free-radical solution terpolymerization of acrylamide, acrylic acid, and acrylonitrile was carried out in a mixture of dimethylformamide and water (60 : 40, v/v) at 85°C using benzoyl peroxide as the initiator. The polymers were characterized by elemental analysis, IR, ¹H-NMR, TGA, and viscosity measurements. Elemental analysis data were used to evaluate the terpolymer composition. The reactivity ratios were determined by Fineman–Ross and Kelen–Tudos methods. The reactivity ratios (*r*) for the copolymerization of (1) acrylic acid + acrylonitrile with (2) acrylamide was found to be $r_1 = 0.86 \pm 0.09$ and $r_2 = 1.93 \pm 0.03$, respectively, by the Kelen–Tudos method. The Fineman–Ross method yielded a value of $r_1 = 0.86 \pm 0.05$ and $r_2 = 1.94 \pm 0.09$, respectively. The activation energy values for various stages of decomposition were calculated from TGA analysis. Voluminosity (V_E) and the shape factor (ν) were also computed from the viscosity measurements in different ratios of the solvent mixture. © 1998 John Wiley & Sons, Inc. *J Appl Polym Sci* 69: 217–228, 1998

Key words: terpolymers; synthesis; properties; reactivity ratio

INTRODUCTION

Research on polymers has been mainly addressed to the synthesis of new materials with specific performance for last 30 years. A wide variety of chemical or physical strategies including copolymerization, polymer blends and composites, or crosslinking networks have been explored to match the individual requirements.¹ Terpolymerizations have continued to evoke interest by both academics and industrialists. One of the main advantages of this technique is that it provides a convenient method of synthesizing new polymeric structures with wide ranges of properties.² Although extensive literature is available for homo- and copolymerization, very little kinetic or synthetic information is available for terpolymerization.³ As it becomes more and more possible to

“tailor-make” polymers with specific physical and chemical properties, it will undoubtedly become necessary to resort to such multiple combinations wherein each monomer contributes some particular property or properties.

Interest in multifunctional synthetic polymers or copolymers is steadily increasing, as macromolecular catalysts, macromolecular drugs, or antimetastatic agents.⁴ Such activated drug-binding matrices are usually based on *N*-acryloyloxyphthalimide and *N*-methacryloyloxyphthalimide with methyl acrylate and acrylonitrile as comonomers. The terpolymerization of maleic anhydride–methyl methacrylate–styrene has been studied extensively and modified by tributyltin oxide to yield terpolymers of biological interest.⁵ The growth in the production of plastic materials during the past few years has been accompanied by an increased demand for materials with improved physical and mechanical properties, greater heat and radiation stability, etc. Only a few homopolymers answer such demands. In this respect, the terpolymerization of acrylonitrile, styrene, and esters of α -cyanocinnamic acid has been

Correspondence to: A. K. Rakshit.

Contract grant sponsor: Department of Biotechnology, Government of India.

Journal of Applied Polymer Science, Vol. 69, 217–228 (1998)

© 1998 John Wiley & Sons, Inc.

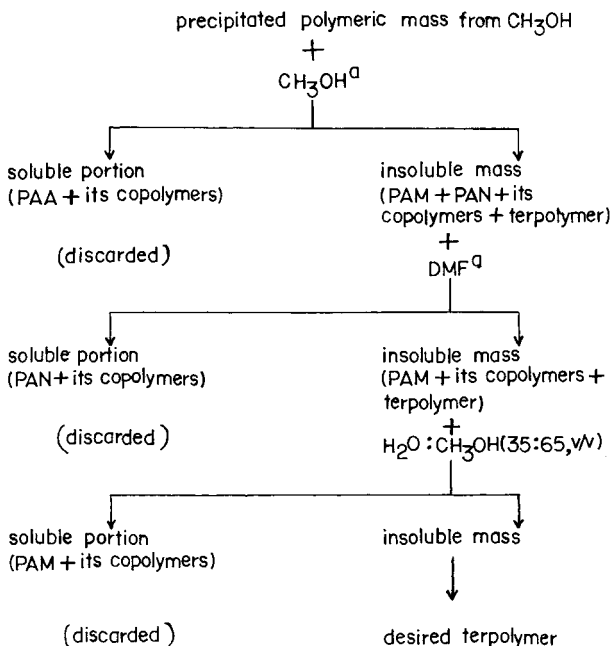
CCC 0021-8995/98/020217-12

reported.⁶ Recently, the water uptake and swelling behavior of physically crosslinked, inhomogeneous poly(acrylonitrile–acrylamide–acrylic acid) hydrogels have been reported.⁷ In this article, we report on the synthesis and properties of terpolymers of acrylamide, acrylonitrile, and acrylic acid from various feed ratios. The changes in the physical and chemical properties as a function of the chemical composition are studied and presented in detail.

EXPERIMENTAL

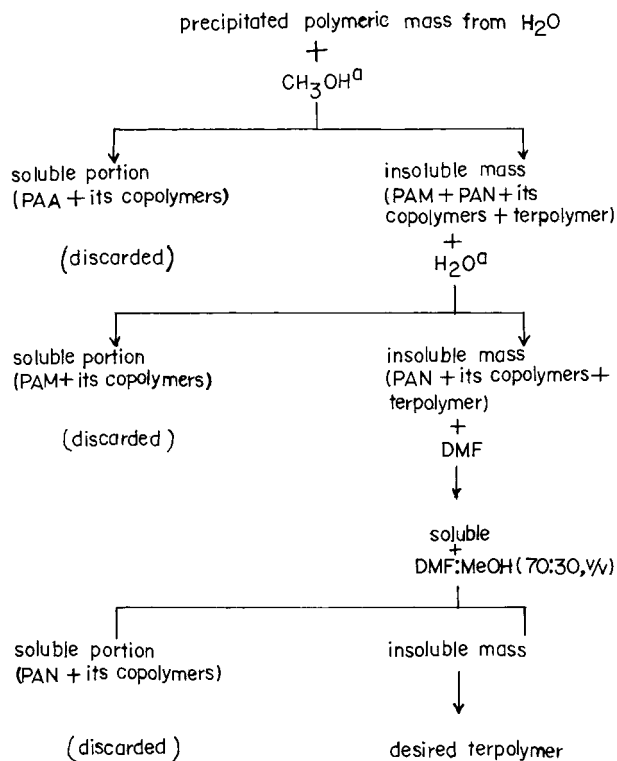
Acrylamide (Mitsubishi Chemicals Ltd.), acrylic acid (National Chemicals, Baroda, India), and acrylonitrile (BDH, Poole, England) were used for the polymerization without any prior purification. Benzoyl peroxide (National Chemicals, Baroda, India) was purified by dissolving it in chloroform at room temperature and reprecipitating it by adding methanol, before it used for the polymerization. Hydrogen peroxide (Glaxo, Mumbai, India, 100 vol, i.e., 30% w/v) was used as received. The solvents were freshly distilled prior to use.

IR spectra of the films of the homopolymers and terpolymers were recorded on a Perkin–Elmer 16PC spectrophotometer. The films were prepared by dissolving the polymer in a mixture of DMF : H₂O (60 : 40, v/v) and pouring the solution



^a soxhlet extraction

Figure 1 Schematic representation of purification of terpolymers I and II.



^a soxhlet extraction

Figure 2 Schematic representation of purification of terpolymers III and IV.

over a pool of mercury. The films were obtained by vacuum evaporation of the solvent.

The NMR of the polymer solutions were recorded on a JEOL GSX, 400 MHz for PMR at the RSIC, IIT, Madras, India. Elemental analysis was done on a Hearaous, RAPID (made in Germany) C, H, N, O, analyzer at S.P. University, Vallabh Vidyanagar, India.

TGA was recorded with a Shimadzu thermal analyzer DT-30B. The TGA analysis was done under a nitrogen atmosphere. Viscosity studies of different solutions were carried out with the help of an Ubbelohde viscometer, placed vertically in a thermostat, at all required temperatures ($\pm 0.05^\circ\text{C}$).

The synthesis of terpolymers was carried out in various monomer feed ratios of (I) 80 : 10 : 10, (II) 60 : 20 : 20, (III) 40 : 30 : 30, and (IV) 20 : 40 : 40 (w/w/w) of acrylamide (AM), acrylic acid (AA), and acrylonitrile (AN), respectively. The solution polymerization was carried out in a mixture of DMF and water (60 : 40, v/v) under a nitrogen atmosphere. The monomer-to-solvent ratio was 1 : 4 (w/v). The initiator benzoyl peroxide concentration was 1.0% (w/w) to total monomer weight. The reactor setup consisted of a three-

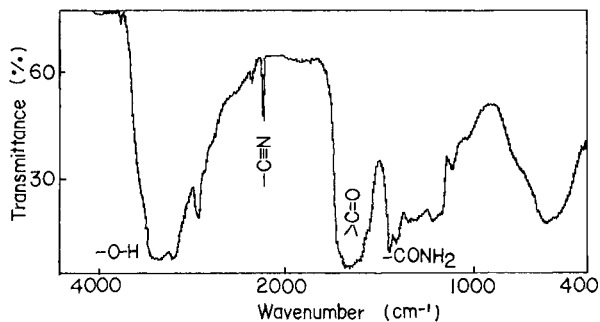


Figure 3 Representative IR spectrum of terpolymer II.

necked round-bottom flask equipped with a water condenser at one side neck and the N_2 inlet at the other. The reaction mixture was mechanically stirred through the center neck. The whole assembly was placed in a thermostated water bath at 85°C . The reaction time was 8 h. After polymerization, the reaction mass, for samples I and II, was poured into an excess of methanol, and for samples III and IV, it was poured into an excess of distilled water. The reprecipitated products were Soxhlet-extracted with various solvents to remove the respective homo- and copolymers. The purification procedure of samples I and II is schematically shown in Figure 1, and that of samples III & IV is shown in Figure 2.

The synthesis of the homopolymers polyacrylic acid (PAA)⁸ and polyacrylamide (PAM)^{9,10} was done as reported in the literature. The synthesis of polyacrylonitrile (PAN) was carried out as reported earlier.^{11,12} All the homo- and terpolymers were dried *in vacuo* and then characterized.

RESULTS AND DISCUSSION

The homopolymers PAM, PAN, and PAA showed characteristic IR absorptions which agreed very well with those reported in the literature. PAN

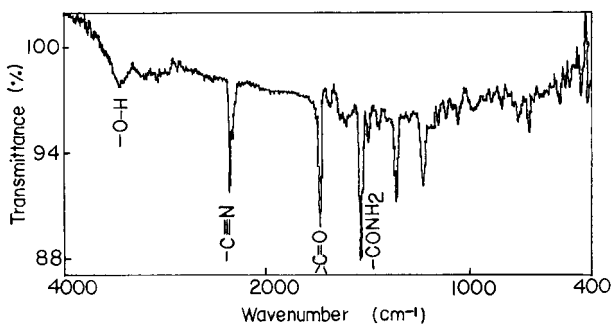


Figure 4 Representative IR spectrum of terpolymer III.

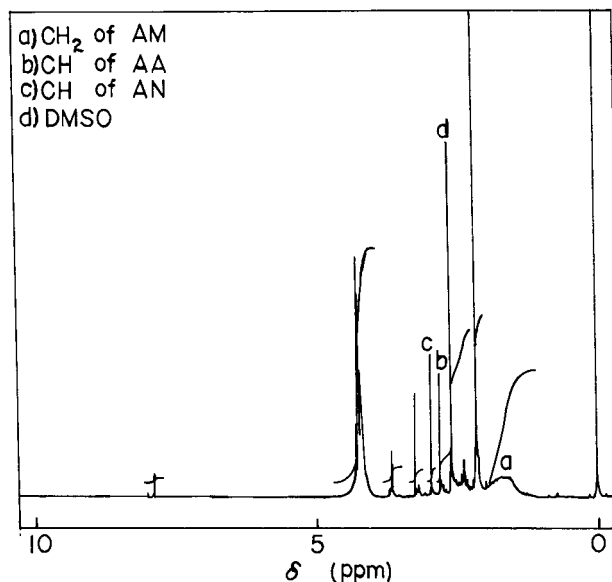


Figure 5 $^1\text{H-NMR}$ spectrum of terpolymer II.

showed strong absorptions at 2246 and 1452 cm^{-1} due to the nitrile group. The $\text{C}=\text{O}$ band of PAA was observed at 1738 cm^{-1} . Besides this, the broad absorption band due to the $\text{O}-\text{H}$ of the $-\text{COOH}$ group was observed around 3300 cm^{-1} . The IR spectrum of PAM showed strong absorption at 1650 cm^{-1} due to the $\text{C}=\text{O}$ bond of the carbonamide group. The medium absorption at 1400 cm^{-1} was due to the $\text{C}-\text{N}$ stretch. Representative IR spectra of terpolymers II (AM : AA : AN = 60 : 20 : 20) and III (AM : AA : AN = 40 : 30 : 30) are given in Figures 3 and 4. The characteristic absorption peaks due to the three functional groups were present in all the terpolymers studied.

Further evidence for the three monomers incor-

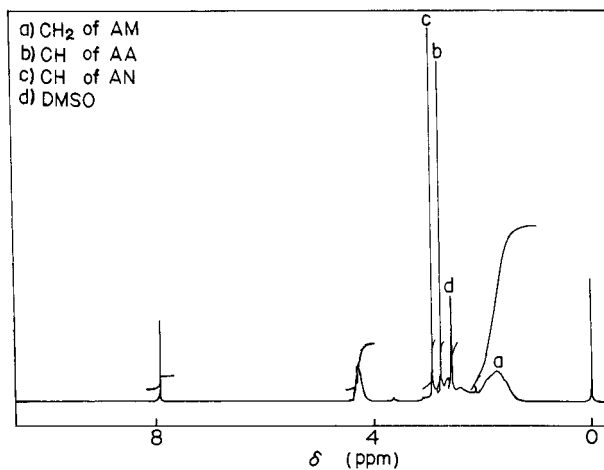


Figure 6 $^1\text{H-NMR}$ spectrum of terpolymer III.

Table I Composition of AM, AA, and AN in Feed and in Terpolymers

Samples	Mol Fraction (M) of AM, AA, and AN in Feed			Elemental Analysis		Mol Fraction (\emptyset) of AM, AA, and AN in Terpolymer (Experimental)		
	(M_{AM})	(M_{AA})	(M_{AN})	N (%)	O (%)	(\emptyset_{AM})	(\emptyset_{AA})	(\emptyset_{AN})
I AM-AA-AN (80 : 10 : 10)	0.775	0.096	0.130	17.14	25.31	0.861	0.130	0.009
II AM-AA-AN (60 : 20 : 20)	0.563	0.185	0.251	17.27	22.18	0.568	0.179	0.254
III AM-AA-AN (40 : 30 : 30)	0.364	0.270	0.366	14.91	24.76	0.446	0.291	0.262
IV AM-AA-AN (20 : 40 : 40)	0.177	0.349	0.474	14.08	23.61	0.224	0.358	0.417
PAM	—	—	—	18.12	25.61	—	—	—
PAN	—	—	—	25.39	—	—	—	—

porated was given by the $^1\text{H-NMR}$ spectra of the terpolymers. In the $^1\text{H-NMR}$ spectra of PAM, the methylene protons appeared as a broad peak at $\delta = 1.6\text{--}1.8$ ppm.¹³ The methine protons resonate at $\delta = 2.28$ ppm. The $^1\text{H-NMR}$ spectrum of PAN shows peaks at $\delta = 2.071$ ppm due to methylene protons and due to methine protons at $\delta = 3.122$ ppm. In the presence of monomer AA, the methylene signal shifted downfield to $\delta = 2.056$; the methine proton also showed a shift to $\delta = 3.120$ ppm.¹⁴ In the case of terpolymers (Figs. 5 and 6), a broad peak appeared in the range of $\delta = 1.4\text{--}2.0$ due to methylene groups of AM. A sharp peak was observed due to the methine of the AA comonomer at $\delta = 2.75$ ppm and at $\delta = 2.93$ due to the AN comonomer. As the ratio of AA and AN increases, the intensity of the peak height increases in the expected direction.

The experimental feed ratios of various monomers as well as the composition of the resulting terpolymers, obtained by elemental analysis, are summarized in Table I. The reactivity ratios (r)

of (AA + AN) and AM in the terpolymer were estimated by the graphical method of Kelen-Tudos¹⁵:

$$\theta = r_1\epsilon - \frac{r_2(1 - \epsilon)}{\gamma} \quad (1)$$

where 1 stands for (AA + AN) and 2 for AM. θ , ϵ , and γ are mathematical functions of G and F as defined in Table II. On plotting θ versus ϵ , a linear plot was obtained. The intercepts at $\epsilon = 0$ and $\epsilon = 1$ gave $-r_2/\gamma$ and r_1 , respectively. The values obtained for r_1 and r_2 were $r_1 = 0.86 \pm 0.09$ and $r_2 = 1.93 \pm 0.03$

The reactivity ratios r_1 and r_2 were also determined by the Fineman-Ross^{16,17} method. The following equation was used:

$$X(Y - 1)/Y = r_1X^2/Y - r_2 \quad (2)$$

where $X = M_1/M_2$ and $Y = \frac{\emptyset_1}{\emptyset_2}$ (as defined in Table II).

Table II Kelen-Tudos Parameters for AM and for AA + AN

Samples	$X = \frac{M_1}{M_2}$	$Y = \frac{\emptyset_1}{\emptyset_2}$	$G = \frac{X(Y - 1)}{Y}$	$F = \frac{X^2}{Y}$	$\epsilon = \frac{F}{\gamma + F}$	$\theta = \frac{G}{\gamma + F}$
I	0.29	0.16	-1.51	0.53	0.23	-0.65
II	0.77	0.76	—	—	—	—
III	1.75	1.24	0.34	2.46	0.58	0.08
IV	4.65	3.46	3.31	6.25	0.77	0.41

$\gamma = \sqrt{F_{\max}F_{\min}} = 1.81$; M_1 is the mol fraction of AA + AN and M_2 is the mol fraction of AM in feed; \emptyset_1 and \emptyset_2 are their respective experimental mol fractions in the terpolymer.

Table III Structural Data for the Terpolymers of AM and of AA + AN

Samples	Composition ^a (Mol Fraction)		Blockiness ^b (Mol Fraction)		Alternation ^b (Mol Fraction)	Mean Sequence Length		$\frac{\mu_1}{\mu_2}$
	θ_1	θ_2	1-1 (X')	2-2 (Y')	1-2 (Z')	μ_1	μ_2	
I	0.14	0.86	0.028	0.748	0.224	1.1	12.9	0.1
II	0.43	0.57	0.215	0.355	0.429	1.6	3.6	0.5
III	0.55	0.45	0.333	0.233	0.433	2.1	2.6	0.8
IV	0.78	0.22	0.624	0.064	0.311	4.1	1.5	2.6

^a From elemental analysis.^b Statistically calculated using reactivity ratios.

On plotting $X(Y - 1)/Y$ against X^2/Y , a straight line was obtained, whose slope was r_1 and the intercept yielded r_2 . The values obtained for r_1 and r_2 are 0.86 ± 0.05 and 1.94 ± 0.09 , respectively. The $r_1 r_2$ value indicates that the terpolymers are block copolymers of AM and (AA + AN) which are rich in AM.¹⁷

The statistical distributions of the monomer sequences 1-1, 2-2, and 1-2 were calculated using the following relations¹⁸⁻²⁰:

$$X' = \theta_1 - 2\theta_1\theta_2 / \{1 + [(2\theta_1 - 1)^2 + 4r_1r_2\theta_1\theta_2]^{1/2}\} \quad (3)$$

$$Y' = \theta_2 - 2\theta_1\theta_2 / \{1 + [(2\theta_1 - 1)^2 + 4r_1r_2\theta_1\theta_2]^{1/2}\} \quad (4)$$

$$Z' = 4\theta_1\theta_2 / \{1 + [(2\theta_1 - 1)^2 + 4r_1r_2\theta_1\theta_2]^{1/2}\} \quad (5)$$

where θ_1 is the mol fraction of AA and AN together and θ_2 is the mol fraction of AM when the blockiness between these are considered in the terpolymers. The mol fractions of 1-1, 2-2, and 1-2 are designated by X', Y', and Z', as listed in Table III. The mean sequence lengths μ_1 and μ_2 were calculated utilizing the relations

$$\mu_1 = 1 + r_1(\theta_1)/(\theta_2) \quad (6)$$

$$\mu_2 = 1 + r_2(\theta_2)/(\theta_1) \quad (7)$$

The calculated values are listed in Table III.

The TGA of PAM, PAA, PAN, and terpolymer

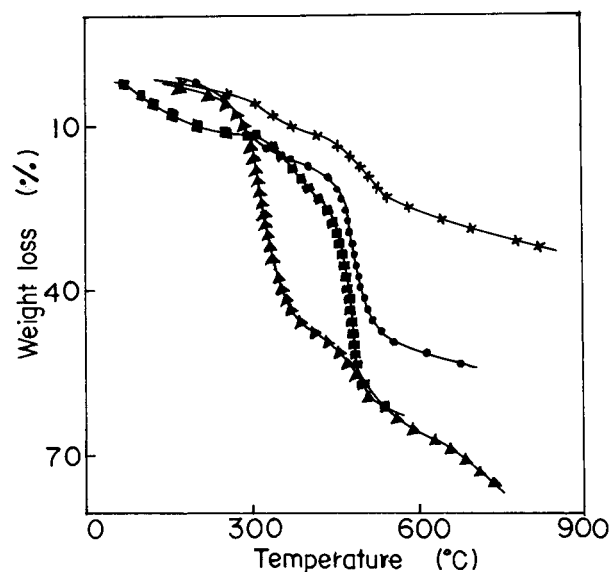


Figure 7 Representative TGA plots of (■) PAM, (▲) PAA, (X) PAN, and (●) terpolymer IV at heating rate of 10 K min^{-1} in N_2 atmosphere.

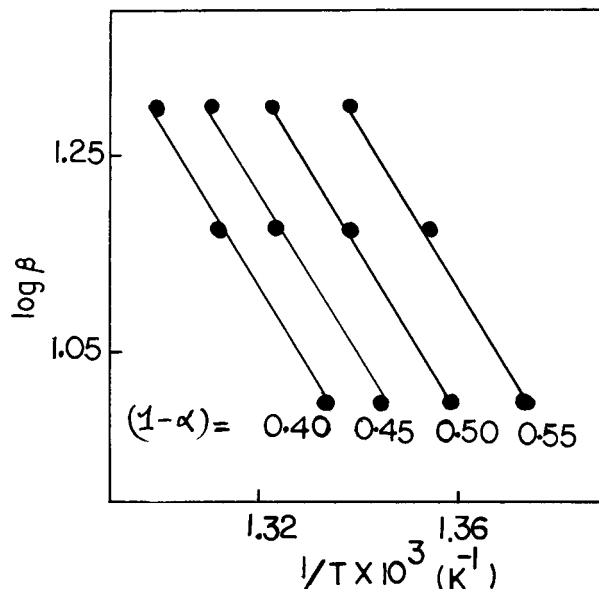


Figure 8 Representative Ozawa plot of $\log \beta$ against $1/T$ for terpolymer IV at different $(1 - \alpha)$ values (see text).

Table IV Activation Energies of Decomposition of Various Homopolymers and Terpolymers (Ozawa Method, See Text)

Polymer Samples		Activation Energy, (E) (kJ mol ⁻¹) ($1 - \alpha$) ^a			
I	AM-AA-AN	61.4	63.6	63.1	60.8
	(80 : 10 : 10)	(0.20)	(0.30)	(0.35)	(0.40)
II	AM-AA-AN	66.1	62.4	59.7	55.5
	(60 : 20 : 20)	(0.20)	(0.25)	(0.30)	(0.35)
III	AM-AA-AN	60.3	57.9	55.3	55.3
	(40 : 30 : 30)	(0.30)	(0.35)	(0.40)	(0.45)
IV	AM-AA-AN	168.8	160.4	152.5	156.9
	(20 : 40 : 40)	(0.40)	(0.45)	(0.50)	(0.55)
	PAM	70.4	70.4	71.3	68.6
		(0.25)	(0.30)	(0.35)	(0.40)
	PAA	69.9	67.5	70.2	67.7
		(0.55)	(0.60)	(0.65)	(0.70)
	PAN	112.1	119.4	112.0	112.0
		(0.20)	(0.30)	(0.35)	(0.40)

^a Values of ($1 - \alpha$) are given in parentheses.

IV are given in Figure 7. The thermogram of terpolymer IV falls in between those of its homopolymers, indicating a somewhat intermediate thermal stability. Other terpolymers also show in-

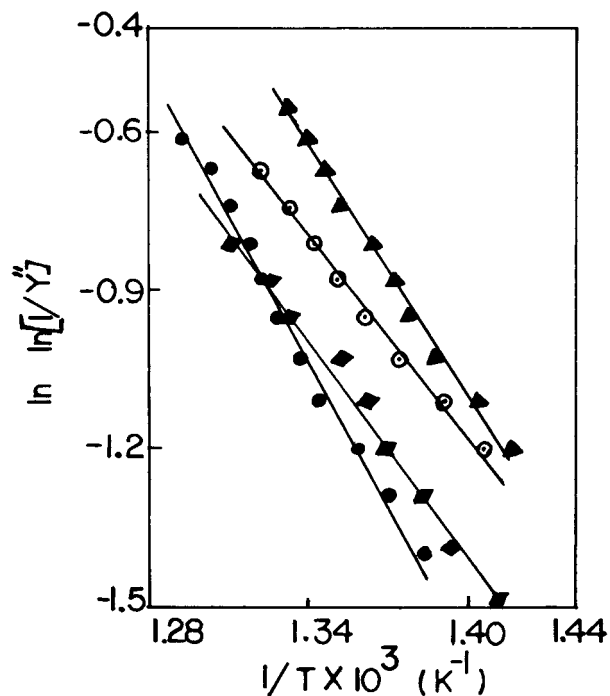


Figure 9 Broido plot for terpolymers: (\blacktriangle) I; (\odot) II; (\blacksquare) III; (\bullet) IV (see text).

intermediate thermal stability. Two-stage decomposition was observed in all cases, except PAM. The first-stage decomposition of PAA started around 260°C. This is due to the formation of anhydride linkages. Similar values were reported earlier for PAA.²¹ Heating above 350°C results in rapid decomposition to monomer, carbon dioxide, and volatile hydrocarbons. The TGA of PAM was three-staged, as observed before.²² First, the loss of water which is nonstoichiometric occurred. This is followed by the subsequent loss of ammonia and other gaseous products from the PAN structure formed during the decomposition of PAM and partly from the remaining PAM in the course of heating to 600°C.²³

The Ozawa²⁴⁻²⁶ method, a dynamic analysis technique, was used for the determination of the activation energy. Thermograms were recorded at various heating rates of 10, 15, and 20 K min⁻¹ in N₂. The fraction of decomposition, α , was obtained by the following equation:

$$\alpha = (W_0 - W_t)/(W_0 - W_f) \quad (8)$$

where W_0 is the initial weight of the polymer; W_t , the weight of the polymer at temperature t ; and W_f , the final weight. The ($1 - \alpha$) values were found for each heating rate from the TG curves; the ($1 - \alpha$) values, hence, obtained were plotted against $1/T$. According to the Ozawa method,²⁴⁻²⁶

Table V Activation Energy of Decomposition for Various Homopolymers and Terpolymers in Different Ratios by Thermogravimetric Analysis

Polymer Samples	Decomposition Temperature Range (°C)	Weight Loss (%)	Activation Energy ^a (kJ mol ⁻¹)
AM : AA : AN (80 : 10 : 10) I	190–425	24	18.0
	433–478	44	65.1
AM : AA : AN (60 : 20 : 20) II	214–399	20	19.9
	439–489	40	48.9
AM : AA : AN (40 : 30 : 30) III	205–410	16	20.3
	436–490	36	58.8
AM : AA : AN (20 : 40 : 40) IV	198–326	14	32.7
	450–501	42	75.0
PAM	70–204	10	20.3
	305–420	24	23.5
	435–495	58	89.2
PAA	260–359	42	66.0
	435–660	70	13.0
PAN	305–473	16	20.3
	520–844	36	11.8

^a Calculated using Broido's method at a heating rate of 10°C/min in N₂ atmosphere.

the plot of $\log \beta$ (where β is the heating rate) against the reciprocal of absolute temperature, for different values of $(1 - \alpha)$, is linear. The activation energy (E) of the decomposition was obtained from the slope of above linear plot,^{24–26} using the equation

$$\text{Slope} = -0.4567 (E/R) \quad (9)$$

The plot of $\log \beta$ versus $1/T$, for terpolymer IV at different values of $(1 - \alpha)$, each differing by 0.05, is shown in Figure 8. The activation energy at different $(1 - \alpha)$ are given in Table IV. For terpolymers, the activation energy of decomposition varied with $(1 - \alpha)$. For homopolymers, the activation energy was independent of the fraction of decomposition. In terpolymer IV, where the AA and AN feed ratios are higher, the E values are much higher than the rest, indicating a synergistic effect on its stability. A high stability of PAN in a nitrogen atmosphere was observed. The PAA and PAM have almost the same stability though lower than PAN in the presence of nitrogen.

The activation energy associated with each stage of decomposition was also evaluated by the well-known Broido method.¹² The equation used for the calculation of activation energy (E) was

$$\ln \ln (1/Y'') = (-E/R)(1/T) + \text{constant} \quad (10)$$

where

$$Y'' = (W_t - W_\infty)/(W_0 - W_\infty) \quad (11)$$

that is, Y'' is the fraction of the number of initial molecules not yet decomposed; W_t , the weight at any time t ; W_∞ , the weight at infinite time (= zero); and W_0 , the initial weight. A plot of $\ln \ln (1/Y'')$ versus $1/T$ [eq. (10)] gives an excellent approximation to a straight line over a range of $0.999 > Y'' > 0.001$. The slope is related to the activation energy. Representative plots are shown in Figure 9. The calculated values for the activation energy of decomposition are listed in Table V. The terpolymers show two-stage decomposition even where AM is 80% in the feed ratio, although the homopolymer PAM shows three-stage decomposition. The first stage of PAM decomposition is not seen in terpolymer decompositions. In general, terpolymers require more activation energy than do the homopolymers.

The viscosity behavior of PAM, PAN, and terpolymers I, II, III, and IV was studied at different temperatures of 30, 35, and 40°C. The viscosity studies of PAM and sets I and II were done in aqueous medium, whereas PAN and sets III and

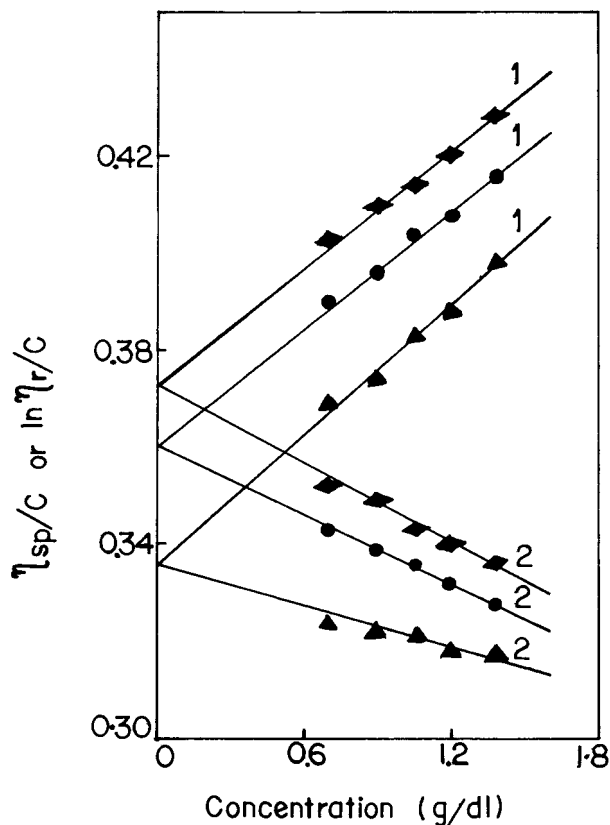


Figure 10 Typical plot of (1) η_{sp}/C and (2) $\ln \eta_r/C$ against concentration (C) for terpolymer IV: (■) 30°C; (●) 35°C; (▲) 40°C.

IV were done in DMF. The viscosity of all the terpolymers was also measured in mixtures of the solvents, that is, various ratios of DMF : H₂O (v/v). The intrinsic viscosity was calculated using the following equations (Huggins and Kraemer):

$$\eta_{sp}/C = [\eta] + K'[\eta]^2C \quad (12)$$

$$\ln \eta_r/C = [\eta] - K''[\eta]^2C \quad (13)$$

where K' and K'' are constants for a given polymer/solvent/temperature system. For many linear flexible polymer systems, K' often indicates the measures of the solvent power; the poorer the solvent, the higher the value of K' . The $K' - K''$ values were found to be around 0.5, as expected.^{27,28}

The η_{sp}/C values of PAM in H₂O, PAN, and set IV in DMF showed a decrease with dilution. When plotted against concentration, straight lines were obtained and intrinsic viscosity values were, hence, computed (Fig. 10). For other systems, η_{sp}/C values showed an increase with dilution, and intrinsic viscosity as well as $K' - K''$ values could not be

calculated. Intrinsic viscosities of various systems at different temperatures and some representative values of $K' - K''$ are given in Table VI.

The viscosities of various terpolymers in water, DMF, and a mixture of water : DMF, like other polyelectrolytes, showed a unique dependence on concentration.²⁹ η_{sp}/C values for the above-mentioned terpolymers increased with dilution, contrary to the behavior of nonionic polymers. Representative plots are shown in Figure 11(a). As the solution is diluted, the polymer molecules no longer fill all the space and the intervening regions extract some of the mobile ions. Net charges develop in the domains of the polymer molecule, causing them to expand. As this process continues with further dilution, the expansive forces increase. At high dilutions, polymer molecules lose most of their mobile ions and are extended virtually to their maximum length.³⁰ This leads to high values of η_{sp}/C . Such data can be satisfactorily handled through the use of the empirical relation

$$\eta_{sp}/C = A/(1 + BC^{1/2}) \quad (14)$$

where A and B are constants. A straight line was obtained on plotting $(\eta_{sp}/C)^{-1}$ against $C^{1/2}$ [Fig. 11(b)], where A represents the intrinsic viscosity $(\eta_{sp}/C)_{C \rightarrow 0}$.³⁰ The plot of $[\eta]$ against the H₂O : DMF ratio (Fig. 12) shows a maximum for all the sets of terpolymers. This indicates that at that maximum of $[\eta]$ the corresponding H₂O : DMF ratio behaves as a good solvent for the terpolymers. Relative viscosity data at different concentrations were used for calculations of the voluminosity (V_E) of the polymer solutions, at a given temperature and in different solvent systems.^{27,28,31} V_E was obtained by plotting Y against concentration C (g dL⁻¹), where (Fig. 13)

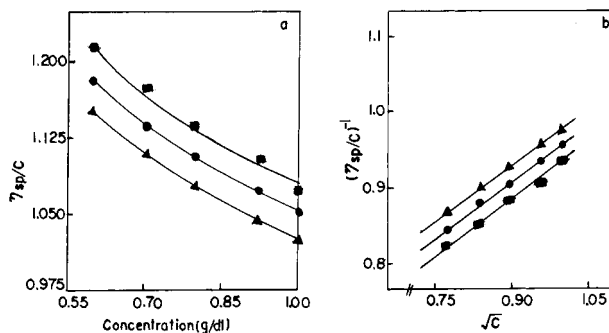


Figure 11 Plot of (a) η_{sp}/C against concentration (C) and (b) $(\eta_{sp}/C)^{-1}$ versus \sqrt{C} for terpolymer I in water: (■) 30°C; (●) 35°C; (▲) 40°C.

Table VI Intrinsic Viscosities of Various Polymer Systems at Different Temperatures in Various Solvents

Polymer Systems/Solvent	A or Intrinsic Viscosity $[\eta]$ (dL/g)			B			$K' - K''$ (40°C)
	30°C	35°C	40°C	30°C	35°C	40°C	
PAM/H ₂ O	—	2.98	2.91	—	—	—	0.51
Set I/H ₂ O	2.19	2.06	1.96	1.02	0.96	0.91	—
/85 : 15 :: H ₂ O : DMF	2.17	2.11	2.09	0.88	0.87	0.88	—
/75 : 25 "	2.21	2.14	2.08	0.99	0.96	0.92	—
/40 : 60 "	2.05	2.03	1.97	1.10	1.08	1.05	—
Set II/H ₂ O	1.33	1.52	1.58	1.04	1.51	1.56	—
/85 : 15 :: H ₂ O : DMF	1.61	1.59	1.57	1.31	1.31	1.28	—
/75 : 25 "	1.72	1.64	1.57	1.42	1.31	1.21	—
/40 : 60 "	1.70	1.59	1.54	1.23	1.33	1.11	—
Set III/DMF	1.11	0.99	0.85	1.32	1.24	0.97	—
/50 : 50 :: H ₂ O : DMF	1.37	1.45	1.48	0.97	1.05	1.13	—
/40 : 60 "	1.58	1.53	1.51	1.11	1.09	1.07	—
/33 : 67 "	1.57	1.53	1.41	1.07	1.09	0.90	—
/25 : 75 "	1.67	1.55	1.45	1.23	1.06	0.97	—
Set IV/DMF	0.37	0.36	0.34	—	—	—	0.48
/33 : 67 :: H ₂ O : DMF	0.33	0.36	0.42	0.22	0.23	0.25	—
/25 : 75 "	0.41	0.35	0.34	0.30	0.09	0.09	—
/15 : 85 "	0.45	0.42	0.40	0.17	0.12	0.07	—
PAN/DMF	0.73	0.72	0.71	—	—	—	0.50

$$Y = (\eta_r^{0.5} - 1) / [C(\eta_r^{0.5} \times 1.35 - 0.1)] \quad (15)$$

$$[\eta] = \nu V_E \quad (16)$$

The straight line then obtained was extrapolated to $C = 0$ and the intercept yielded V_E . The values are listed in Table VII. The shape factor ν was calculated from the equation

The shape factor gives an idea of the shape of the macromolecules in the solution.³² The values of the shape factors obtained are given in Table VII. All the values for systems behaving normally

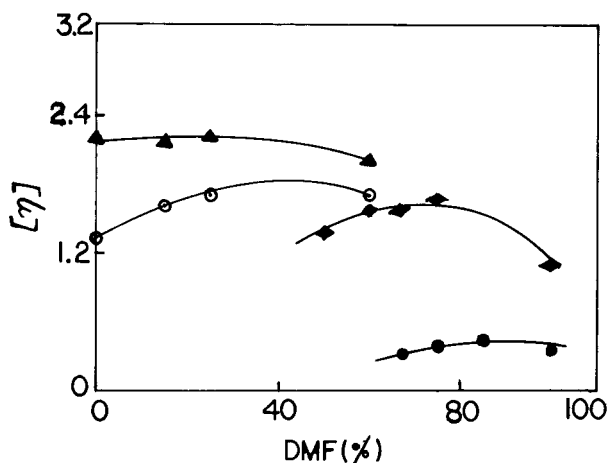


Figure 12 Plot of intrinsic viscosity $[\eta]$ versus percentage DMF for terpolymers: (▲) I; (○) II; (■) III; (●) IV.

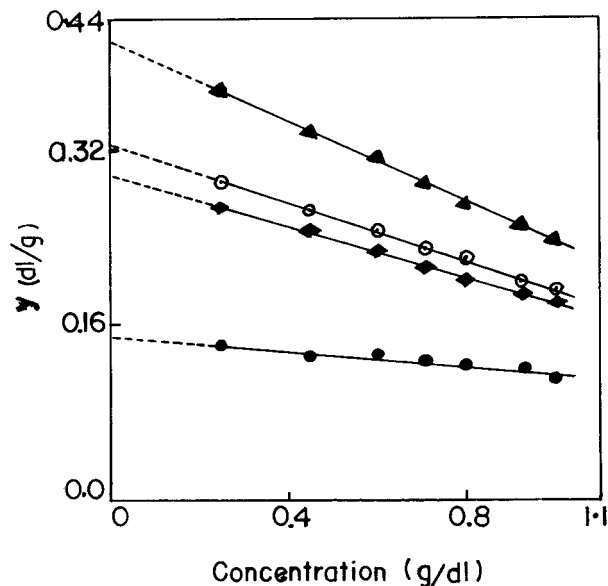


Figure 13 Plot of y versus concentration (C) for terpolymers: (▲) I in water; (⊙) II in DMF : H₂O (60 : 40); (■) III in DMF : H₂O (50 : 50); (●) IV in DMF.

(PAM in H₂O, PAN and set IV in DMF) were found to be around 2.5, indicating a spherical conformation³³ of the macromolecules in the solution. The ν values as shown in Table VII were found

to be independent of temperature (varying between 2.5 and 2.6), indicating that the minor axis varies by about 1%. The rest of the systems gave a higher value of ν due to both the complicated distribution in the solution of highly elongated chains and also because of their electrostatic interactions when highly charged. The change in the property of the polymer solution with a change in temperature depends on two antagonistic factors: (i) coiling/uncoiling of polymer chains and (ii) change in the degree of rotation about a skeletal bond.³⁴ The first one changes the length of the chain, and with increase in temperature, generally increases, leading to higher $[\eta]$ or higher ν . The second one increases the degree of rotation with increase in temperature and thereby should decrease $[\eta]$ and, hence, ν . From Table VII it can be seen that the shape factor ν , in general, somewhat decreases, that is, it is oblate spheroid³³ for almost all systems with increase in temperature, indicating a tendency toward spherical conformation at higher temperature.

The voluminosity V_E (dL/g) is a function of temperature and is a measure of the volume of solvated polymer molecules.³¹ As the temperature increases, desolvation takes place and, hence, V_E decreases. In our systems also, V_E values decrease

Table VII Voluminosity (V_E) and Shape Factor (ν) of Various Polymers at Different Temperatures

Polymer Systems/Solvent	30°C		35°C		40°C	
	V_E (dL/g)	ν	V_E (dL/g)	ν	V_E (dL/g)	ν
PAM/H ₂ O	—	—	1.160	2.5	1.17	2.5
Set I/H ₂ O	0.421	5.2	0.411	5.0	0.403	4.9
/85 : 15 :: H ₂ O : DMF	0.438	4.9	0.430	4.9	0.420	4.9
/75 : 25 "	0.428	5.2	0.424	5.0	0.421	5.0
/40 : 60 "	0.394	5.2	0.393	5.2	0.388	5.1
Set II/H ₂ O	0.312	4.3	0.315	4.8	0.316	5.0
/85 : 15 :: H ₂ O : DMF	0.309	5.2	0.304	5.2	0.304	5.2
/75 : 25 "	0.314	5.5	0.313	5.2	0.311	5.0
/40 : 60 "	0.326	5.2	0.321	5.0	0.316	4.9
Set III/DMF	0.235	4.7	0.221	4.4	0.206	4.1
/50 : 50 :: H ₂ O : DMF	0.298	4.6	0.308	4.7	0.303	4.9
/40 : 60 "	0.320	4.9	0.316	4.8	0.314	4.8
/33 : 67 "	0.322	4.9	0.315	4.9	0.313	4.5
/25 : 75 "	0.325	5.2	0.321	4.8	0.314	4.6
Set IV/DMF	0.151	2.5	0.146	2.5	0.136	2.5
/33 : 67 :: H ₂ O : DMF	0.115	2.9	0.124	2.9	0.139	3.0
/25 : 75 "	0.135	3.0	0.128	2.7	0.126	2.5
/15 : 85 "	0.156	2.9	0.152	2.8	0.147	2.7
PAN/DMF	0.282	2.6	0.277	2.5	0.270	2.6

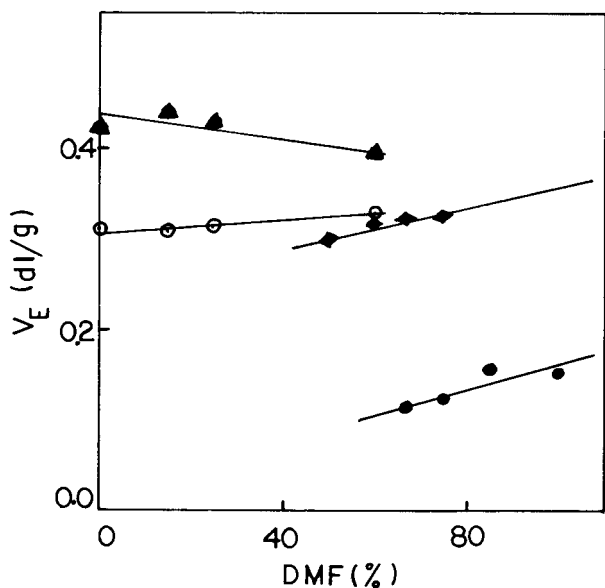


Figure 14 Plot of voluminosity (V_E) versus percentage DMF for terpolymers. Symbols as in Figure 13.

with increase in temperature, indicating desolvation as shown in Table VII. For the highly water-soluble terpolymer of set I, the V_E decreases as the DMF concentration in the mixed solvent increases. For set II, which is partially water-soluble, V_E increases with increasing percent DMF composition. The same was observed for sets III and IV (Fig. 14). For set I which is water-soluble, the DMF : water mixture acts as a poor solvent because the V_E value decreases with increase in DMF concentrations. For other sets of polymers (II, III, and IV) which are partially water-soluble or -insoluble, the DMF : water mixture is a good solvent to a certain extent since V_E is found to increase with increasing DMF content.

CONCLUSION

On the basis of these results, it can be concluded that the free-radical terpolymerization reactions of acrylamide, acrylic acid, and acrylonitrile systems studied follow classic copolymerization theory. The higher reactivity of acrylamide than that of the other two monomers taken together were supported by the reactivity ratios. IR and $^1\text{H-NMR}$ spectroscopy provided evidence for the structure of the terpolymers and activation energies as well as the shape factors of the terpolymers that were obtained by TGA and solution viscosity studies.

The authors thank the Department of Biotechnology, Government of India, for financial assistance. They also thank the S.P. University, Vallabh Vidyanagar, for the elemental analysis.

REFERENCES

1. X. Jin, C. Carfagna, L. Nicolais, and R. Lanzetta, *Macromolecules*, **28**, 4785 (1995).
2. P. Shukla and A. K. Srivastava, *Polymer*, **35**, 4665 (1994).
3. P. Shukla and A. K. Srivastava, *Macromol. Rep., A*, **31**, 315 (1994).
4. A. A. Mahmoud, A. F. Shaaban, A. A. Khalil, and N. N. Massiha, *Polym. Int.*, **27**, 333 (1992).
5. G. Kysela and E. Staudner, *J. Polym. Mater.*, **9**, 297 (1992).
6. S. H. Ronel and D. H. Kohn, *J. Appl. Polym. Sci.*, **19**, 2359 (1975).
7. D. S. G. Hu and M. T. S. Lin, *Polymer*, **35**, 4416 (1994).
8. A. S. Teot, in *Encyclopedia of Chemical Technology*, Vol. 20, M. Grayson, Ed., Wiley, New York, 1980, p. 217.
9. J. D. Morris and R. J. Penzenstadler, in *Encyclopedia of Chemical Technology*, Vol. 10, M. Grayson, Ed., Wiley, New York, 1980, p. 321.
10. W. M. Thomas, in *Encyclopedia of Polymer Science and Technology*, Vol. 1, H. F. Mark, N. G. Gaylord, and N. M. Bikales, Eds., Wiley, New York, 1964, p. 181.
11. R. Joseph, S. Devi, and A. K. Rakshit, *J. Appl. Polym. Sci.*, **50**, 173 (1993).
12. A. Broido, *J. Polym. Sci.*, **7**, 1761 (1969).
13. F. Candau, Z. Zekhnini, F. Heatley, and E. Franta, *Colloid Polym. Sci.*, **264**, 676 (1986).
14. P. Bajaj, K. Sen, and S. Hajar Bahrami, *J. Appl. Polym. Sci.*, **59**, 1539 (1996).
15. T. Kelen and F. Tudos, *J. Makromol. Sci. Chem.*, **9**, 1 (1975).
16. M. Fineman and S. Ross, *J. Polym. Sci.*, **5**, 259 (1980).
17. N. A. Granem, N. A. Massiha, N. E. Ikladious, and A. F. Shaaban, *J. Appl. Polym. Sci.*, **26**, 97 (1981).
18. C. L. McCormick and G. S. Chen, *J. Polym. Sci.*, **22**, 3633, 3649 (1984).
19. C. L. McCormick and K. P. Blackmon, *Polymer*, **27**, 1971 (1986).
20. S. Igarshi, *J. Polym. Sci. Polym. Lett. Ed.*, **1**, 359 (1963).
21. D. H. Grand and N. Grassie, *Polymer*, **1**, 125 (1960).
22. L. M. Minsk, C. K. Chik, G. N. Meyer, and W. O. Kenyon, *J. Polym. Sci. Polym. Ed.*, **12**, 133 (1974).
23. M. Tutas, M. Saglam, M. Yuksel, and C. Guler, *Thermochim. Acta*, **111**, 121 (1987).
24. T. Ozawa, *J. Therm. Anal.*, **2**, 301 (1970).
25. T. Ozawa, *Bull. Chem. Soc. Jpn.*, **38**, 1881 (1965).

26. H. Nishizaki, K. Yoshida, and J. H. Wang, *J. Appl. Polym. Sci.*, **25**, 2869 (1980).
27. V. Vangani and A. K. Rakshit, *J. Appl. Polym. Sci.*, **45**, 1165 (1992).
28. R. Joseph, S. Devi, and A. K. Rakshit, *Polym. Int.*, **26**, 89 (1991).
29. T. Ogawa and M. Sakai, *J. Appl. Polym. Sci.*, **23**, 2817 (1979).
30. P. J. Flory, *Principles of Polymer Chemistry*, 1st ed., Cornell University Press, New York, 1953, p. 635.
31. S. Ajitkumar, D. Prasadkumar, S. Kansara, and N. K. Patel, *Eur. Polym. J.*, **31**, 149 (1995).
32. H. H. Kohler and J. Strand, *J. Phys. Chem.*, **94**, 7628 (1990).
33. G. V. Vinogradov and A. Ya. Malkin, *Rheology of Polymers*, Mir, Moscow, 1980.
34. M. Bhagat, S. Joshi, S. S. Kansara, and N. K. Patel, *J. Polym. Mater.*, **14**, 159 (1997).